Journal of Hydrology 458–459 (2012) 9–15

Contents lists available at SciVerse ScienceDirect

Journal of Hydrology

journal homepage: www.elsevier.com/locate/jhydrol

# Flow dynamics and age stratification of freshwater lenses: Experiments and modeling

Leonard Stoeckl *, Georg Houben

*Federal Institute for Geosciences and Natural Resources, BGR, Stilleweg 2, 30655 Hannover, Germany*

ARTICLE INFO

*Article history:*
Received 22 March 2012
Received in revised form 21 May 2012
Accepted 30 May 2012
Available online 19 June 2012
This manuscript was handled by Peter K. Kitanidis, Editor-in-Chief, with the assistance of Jian Luo, Associate Editor

*Keywords:*
Freshwater lens
Variable-density flow
Physical model
Age stratification
Upconing

SUMMARY

The development and flow dynamics of freshwater lenses are investigated by physical experiments on a laboratory scale. Using an acrylic glass box and a combination of different tracers we were able to simulate a cross section of an infinite strip island and visualize its groundwater flow patterns. For validating our model, results of the generation and degeneration of the freshwater lens were compared to analytical and numerical models. Using recharge water of different colors we were able to visualize flow paths as well as the age stratification within a freshwater lens. Flow paths in the lens could be demonstrated to remain in contact to the outflow zone at all times during the experiments. Analytical solutions are in good accordance to our findings. Additional experiments show the differences between pumping from a horizontal and a vertical well on the interface. These experiments with identical boundary conditions confirm former presumptions: A horizontal well shows less up-coning of the interface and therefore allows a higher sustainable yield than a vertical well.



## 1. Introduction

About half of the worlds population lives within 100 km of the oceanic coast and an increase by population growth and migration is predicted for 2025 (PAI, 2006). In coastal zones and on oceanic islands, fresh groundwater is usually separated from the underlying saline groundwater due to different densities. The resulting freshwater bodies, on islands called lenses, are often the only resource for freshwater supply. Increasing stress on freshwater sources due to climate change, population growth, and increasing industrial and agricultural water demand therefore endangers water supply in many parts of the world (e.g. Maas, 2007; Oude Essink, 1996; Oude Essink et al., 2010). Non-sustainable use potentially incurs the intrusion of saltwater. The cone of depression of a vertical well decreases the height of the freshwater column above the interface. This can lead to upconing and in the worst case to intrusion of saltwater into the well (Dagan and Bear, 1968; Schmorak and Mercado, 1969; Gupta and Gaikwad, 1988; Zhou et al., 2005). Horizontal wells (radial collector wells), on the other hand, distribute drawdown more evenly and may thus be an alternative to vertical wells.

Literature on the interaction of freshwater and saline water in coastal zones and on oceanic islands is abundant. A good overview can be found e.g. in Cooper et al. (1964), Bear et al. (2010) and Werner et al. (in press). Starting from the fundamental hydrostatic studies by Baydon-Ghyben (1898) and Herzberg (1901), recent decades have seen the development of a multitude of methods and models. Geophysical methods, mainly geoelectrical and electromagnetic techniques, both airborne and from the ground, allow delineating the distribution of salt and freshwater and locating the interface that separates both (e.g. Tronicke et al., 1999; Barrett et al., 2002; Siemon et al., 2009). Analytical models to calculate the geometry of lenses were developed by e.g. Fetter (1972), van der Veer (1977), Vacher (1988), Stuyfzand and Bruggeman (1994) and White and Falkland (2010). Vacher et al. (1990) and Chesnaux and Allen (2008) derived analytical solutions to predict residence and travel times, respectively. A variety of numerical studies of variable density flow has been published (e.g. Oberdorfer et al., 1990; Michael et al., 2005; Bailey et al., 2009).

Physical models remain important tools to gain information about fresh and saltwater interaction and the effects of groundwater extraction by wells on the interface, for example by upconing (e.g. Simmons et al., 2002; Zhang et al., 2002; Oswald and Kinzelbach, 2004; Goswami and Clement, 2007; Werner et al., 2009; Abdollahi-Nasab et al., 2010; Jakovovic et al., 2011; Luyun et al., 2011; Shi et al., 2011). Physical models of freshwater lenses, however, are scarce. Pennink (1915) and Zhao et al. (2009) performed experiments visualizing lens generation and upconing.

Except for the analytical models by Vacher et al. (1990) and Chesnaux and Allen (2008) little information is available on the internal flow dynamics and age stratification of freshwater lenses.

* Corresponding author. Tel.: +49 511 643 3375.
*E-mail address:* leonard.stoeckl@bgr.de (L. Stoeckl).

0022-1694/$ - see front matter © 2012 Elsevier B.V. All rights reserved.
http://dx.doi.org/10.1016/j.jhydrol.2012.05.070

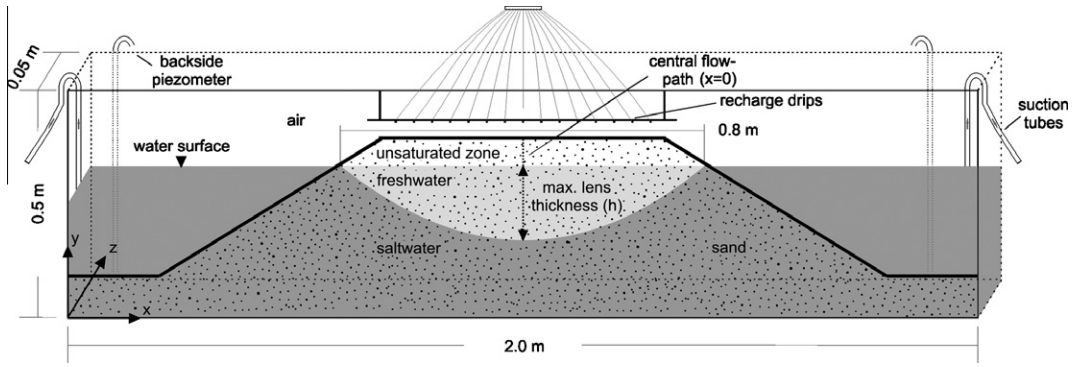


**Fig. 1.** Sketch of the sand box model used for the physical experiments.

Our study aims at filling this gap. We have performed a series of physical models to study the time-dependent formation and degradation of lenses, flow paths and travel times, internal age stratification and the upconing caused by vertical and horizontal wells, respectively. Three techniques using colored dyes were employed to visualize internal flow dynamics: (1) spatial variation of recharge water color during one infiltration event to visualize flow paths, (2) time-dependent (step-wise) variation of recharge water color in order to visualize age stratification, (3) introducing spots of colored water into the saline zone to visualize its movements. All scenarios were numerically simulated and compared to analytical solutions.

## 2. Experimental methods and materials

### 2.1. Physical model

We used an acrylic glass box of 2.0 m in length, 0.5 m in height and 0.05 m in thickness for our experiments. A cross section of an infinite strip island was simulated by filling coarse sand into the box, forming a homogeneous sand cone (Fig. 1). The sand was slightly compacted by palpitation. The grain size distribution (sieve curve) of the filter gravel ($d \approx 0.7$–$1.2$ mm) used in all experiments was optically determined using a Camsizer by Retsch Technology, Germany, with a measurement range between 30 µm and 30 mm. Hydraulic conductivity was determined applying the empirical formula by Beyer and Schweiger (1969) on the measured sieve curves, assuming medium compaction. Together with additional DARCY conductivity tests, a mean hydraulic conductivity $K$ of $4.5 \times 10^{-3}$ m s$^{-1}$ was obtained. According to Beyer and Schweiger (1969) total porosity was determined to be 0.39.

Density of water was determined using a density meter DMA 38 by Anton Paar, Austria. Freshwater density was determined to be 997.4 kg m$^{-3}$. Saltwater (uncolored) with a density of 1021.2 kg m$^{-3}$, simulating ocean water, was injected, saturating the sand from the bottom. Prior to injection, the saltwater was degassed to prevent air from being entrapped in pores. The temperature of the salt and freshwater as well as the air temperature in the laboratory was monitored and kept stable throughout the experiment (23 °C).

To simulate recharge, fifteen individual freshwater drips were installed above the sand cone, connected to an BVP peristaltic pump by Ismatec, Wertheim, Germany (Fig. 1). For visualization, the tracer dyes uranine (yellow[1]), eosine (red) and indigotine (blue), respectively, were added to the freshwater at a concentration of 0.3 g l$^{-1}$. It was assumed that effects of the tracers on density and viscosity of the fluid can be neglected.

Freshwater discharging into the "ocean" formed a thin layer on top of the free saltwater surface. It was continuously skimmed from the left and right boundary of the model by a peristaltic pump with a rate equaling total freshwater recharge. This prevents dilution of saltwater and maintains a constant water level. Slight mixing due to diffusion and dispersion was visible but we were able to show, by measuring saltwater conductivity, that this has no significant effect on saltwater density. Small fluctuations in the water table did not cause any significant deviations. The skimming might be replaced in future experiments by adding saltwater reservoirs to both sides of the model, similar to the set-up used by Zhang et al. (2002) and Luyun et al. (2011).

The specific electrical conductivity of water pumped from the model wells was continuously measured using a TetraCon DU/T flowthrough conductivity probe and a MultiLine P4 conductivity meter, both by WTW GmbH, Weilheim, Germany. Values were stored (5 s interval) on a laptop using the software MultiLab Pilot (WTW). The electric conductivity of the freshwater (tap water plus tracer) was 590 µS cm$^{-1}$. For a detailed optical analysis, all experiments were filmed at an interval of one picture per second (Sony XD CAM-EX).

When interpreting the physical models some general restrictions have to be taken into account:

(1) The ratio of the freshwater lens thickness to the width of the island is rather high in our physical model, around 0.15 m/0.8 m ≈ 1:5. Vacher (1988) describes ratios between 1:30 and 1:100 for real lenses. For some of the Friesian Islands off the German North Sea shore, we calculated ratios between 1:20 and 1:60, using the smallest widths of these elongated barrier islands. Flow processes in our physical model are therefore affected by an at least tenfold vertical exaggeration. The Dupuit assumption of horizontal flow within the lens, as applied in many analytical models, is thus violated to some degree, especially far from the coast.

(2) In our physical model, a capillary fringe inevitably developed above the water level. Such a fringe can also be found in real freshwater lenses but is of much less importance there, as the fringe usually constitutes only a small percentage of the thickness of the unsaturated zone. In our model, the measured fringe thickness covers almost the entire unsaturated zone. Flow in the unsaturated zone was therefore not considered in our numerical modeling.

(3) Our physical model is not strictly two dimensional because of its thickness of 5 cm. Nevertheless, simulating homogeneous recharge and groundwater flow of such a slice of an infinite strip island is still possible without significant deviations from reality. In the case of a singularity, e.g. a pumping well, flow becomes three-dimensional. In that case, boundary effects of the walls will lead to deviations of the mathematical models from the observed results.

[1] For interpretation of color in Figs. 2, 7 and 8, the reader is referred to the web version of this article.

(4) Reading off values from the film recordings of the experiments has an accuracy of about one centimeter due to uneven recharge pattern and dispersion of colors during transport.

### 2.2. Analytical models

The maximum thickness $h$ (L) of an infinite strip oceanic freshwater lens in a single layer aquifer can be calculated using the formula by Fetter (1972):

$$h^2 = \frac{R(L^2 - x^2)}{K(1+\alpha)} \quad (1)$$

where $R$ is the recharge rate ($L\,T^{-1}$), $L$ the half width of the island (L), $x$ the horizontal distance from the island centre (in our case $x = 0$) (L), $K$ the hydraulic conductivity ($L\,T^{-1}$) and $\alpha$ the Ghyben-Herzberg factor (Baydon-Ghyben, 1898; Herzberg, 1901):

$$\alpha = \frac{\rho f}{\rho s - \rho t} \quad (2)$$

where $\rho_s$ ($M\,L^{-3}$) and $\rho_f$ ($M\,L^{-3}$) are the density of salt and freshwater, respectively. Vacher (1988) presented a very similar formula to calculate the maximum thickness $h$ (L) of a freshwater lens:

$$h^2 = \frac{R(\alpha+1)L^2}{K} \quad (3)$$

The transient development of the thickness of a freshwater lens can be calculated using the analytical model proposed by Stuyfzand and Bruggeman (1994), based on work by Brakel (1968) and Bakker (1981), both cited in Stuyfzand and Bruggeman (1994).

$$t = \frac{f_1 \cdot f_2}{2} \cdot \sqrt[-2]{\left[\frac{4 \cdot R \cdot K \cdot (\rho_s - \rho_f)}{(n_e \cdot B)^2 \cdot \rho_s}\right]} \cdot \ln\left[\frac{1 + \frac{Z_t}{Z_\infty}}{1 - \frac{Z_t}{Z_\infty}}\right] \quad (4)$$

where $B$ is the width of the dune belt (here $B = 2L$) (L), $Z_t$ is the depth to the interface at time $t = t$, $Z_\infty$ is the same at $t = \infty$ (steady state), $f_1$ is a correction factor to account for aquifer anisotropy, here $f_1 = 1$ (see Stuyfzand and Bruggeman (1994) for a detailed description), $f_2$ is a correction factor to improve fit to a numerical model by Bakker (1981, cited in Stuyfzand and Bruggeman, 1994), here $f_2 = 1$.

For infinite strip islands, the formula to calculate travel times $t$ in an unconfined horizontal aquifer as a function of the horizontal location $x$ by Chesnaux and Allen (2008) is:

$$t(x) = n_e \sqrt{\frac{\rho_f + \Delta\rho}{R \cdot K \cdot \Delta\rho}} \cdot \left[\sqrt{L^2 - x^2} - \sqrt{L^2 - x_i^2} - L \cdot \ln\left(\frac{L + \sqrt{L^2 - x^2}}{L + \sqrt{L^2 - x_i^2}} \frac{x_i}{x}\right)\right] \quad (5)$$

where $n_e$ is the effective porosity, $\Delta\rho = \rho_s - \rho_f$ and $x_i$ the initial position on the island ($x_i > 0$).

### 2.3. Numerical model

For numerical modeling the finite element model FEFLOW 5.4 was used (Diersch, 2005). A two dimensional model with parameters and boundary conditions based on the setup of the physical model was generated. A trapezoidal mesh with 112,528 elements and 56,791 nodes was used. The grid was refined in the middle of the model at its axis of symmetry and around the wells to avoid numerical dispersion. The upper boundary of the mesh was assigned a Neumann (constant flux) boundary condition, allowing only freshwater to enter the model. An unsaturated zone was not considered for the reasons mentioned above.

The coastal zones were defined as Dirichlet boundaries (constant head) with a saltwater head of 0.3 m (upper model boundary). Considering the cell sizes and the short flow path lengths in the range of a few centimetres, longitudinal and transversal dispersivities were set to $5 \times 10^{-3}$ m and $5 \times 10^{-4}$ m, respectively. The molecular diffusion coefficient was set to $10^{-9}$ $m^2\,s^{-1}$, although the elevated flow velocities in our model render diffusion negligible.

The discretization in time allowed an automatic adaption of the time-step during the model run. Initial time step length was set to 0.864 s, with a maximum ratio for changing the time-step size (new/old) of 1.3 and an upper bound of 8.64 s.

In the case of a pumping well, the model was expanded to a three dimensional model. Six layers with a spacing of 1 cm in the $z$ direction were duplicated from the two dimensional model grid with identical flow and transport parameters.

## 3. Results

### 3.1. Steady state lens thickness as a function of recharge

In the first experiment, the influence of recharge rates on the maximum steady state lens thickness in the middle of the "island" ($x = 0$) was investigated. Our physical model results were compared to analytical models by Fetter (1972) and Vacher (1988), as well as to a numerical FEFLOW model (Fig. 2).

Both analytical models yield, as expected, almost identical results, with the numerical calculations being in good accordance (Fig. 2). Our physical model results match the predicted lens thicknesses well. The slight deviations can be attributed to observational inaccuracies.

The comparison of the FEFLOW simulations to the analytical models and the results from the sand box experiments show, that the numerical code can successfully simulate the results of the physical models.

### 3.2. Transient lens genesis and degradation

By applying a constant freshwater recharge rate of 0.046 $m^3\,d^{-1}$ (1.152 $m\,d^{-1}$) to our physical model, a lens developed and reached dynamical equilibrium after around 200 min (Fig. 3a, see also Video 1, Supplementary material). At this quasi steady state condition, a maximum thickness of 15 cm below the original salt water level was observed. At the end of the first stage of this experiment, recharge was turned off and the degradation of the lens was monitored (Fig. 3b; Video 2, Supplementary material). To maintain

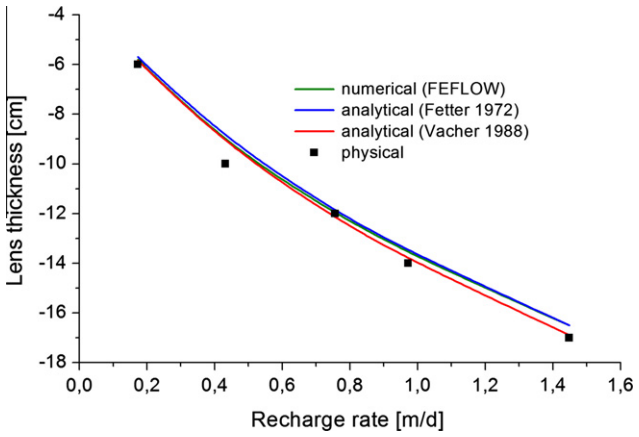


**Fig. 2.** Maximum lens thickness at $x = 0$ under steady state conditions as a function of recharge rate from physical, analytical and numerical models.

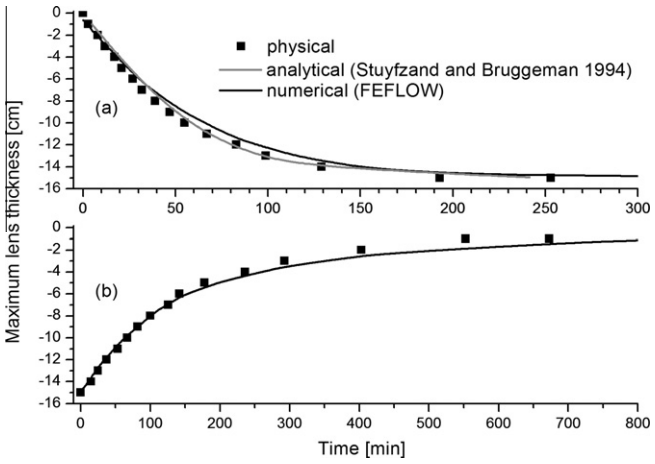


**Fig. 3.** Physical, analytical and numerical results of lens thickness at $x = 0$ as a function of time for (a) freshwater lens formation at recharge rate $R = 1.152$ m d$^{-1}$ and (b) freshwater lens degradation after turning off recharge.

the boundary conditions during this stage, saltwater inflow into the model had to be enabled. This was done with a rate of 0.96 m d$^{-1}$, through the backside piezometer (Fig. 1) at the lower right and left corner of the model.

Fig. 3a shows that the transient development of the lens thickness at $x = 0$ is in good accordance to the analytical and numerical simulation results. No calibration of the initial hydraulic parameters was needed. The degradation of the lens, on the other side, could be simulated only by the numerical model, as no analytical model is available. The curve fit is good (Fig. 3b). It has to be considered, though, that in the physical model, water continues to seep from the unsaturated zone after turning off re-charge for some time, thereby retarding the process of lens degradation.

The two different shapes (velocities) of the generation (Fig. 3a) and degradation curves (Fig. 3b) can be explained by differences in the hydraulic driving forces for each phase. The main difference is the active recharge during the formation of the lens while during degradation this force is not active.

### 3.3. Flow paths and travel times

We were able to visualize flow paths within the freshwater lens by switching the color of every second recharge drip point (indigotine/eosine) in periodic intervals, while all other drips remained on uranine. This was done after equilibrium between fresh and saltwater had been established (Video 3, Supplementary material). As shown in Fig. 4 all flow paths are connected to the discharge zones to the left and right side of the island. Due to the exaggeration of the lenś thickness in comparison to its width, the vertical flow component is clearly visible.

The travel times along the flow paths were measured (Fig. 4). Results are shown in Fig. 5 and compared to calculations based on the analytical model (formula 5) by Chesnaux and Allen (2008) and numerical simulation results with FEFLOW.

The differences between the physical data and the curves for the analytical and the numerical models shown in Fig. 5 are quite minor. They can be attributed to the limited observational accuracy. Even the fact that the analytical model considers only horizontal flow, based on the Dupuit assumption, while in our model a vertical flow component is clearly visible, is apparently not of concern.

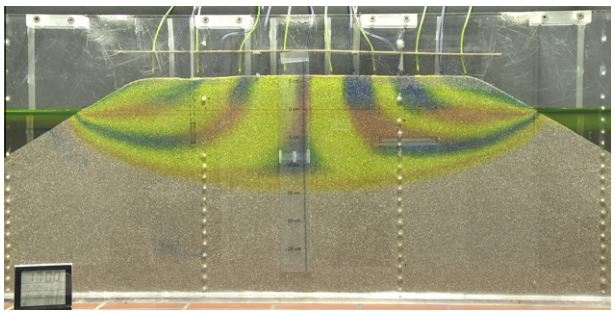

**Fig. 4.** Sand-box model visualizing flow paths with color variations of 60 min duration at every second recharge drip (well inactive).

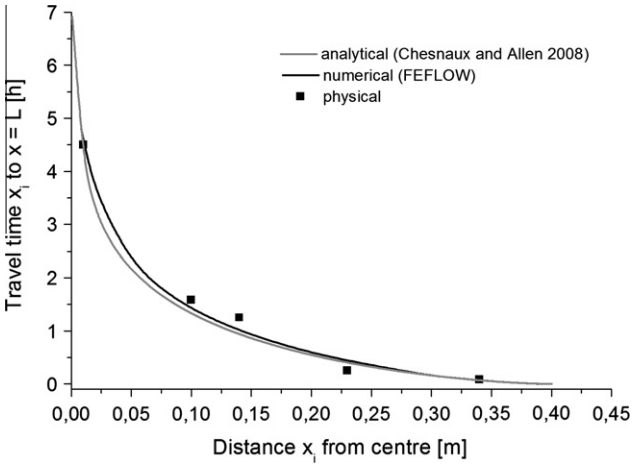


**Fig. 5.** Comparison of travel times as a function of distance from the island centre from physical, analytical and numerical models.

### 3.4. Age stratification

Age dating of water in subsurface hydrology is used to e.g. calculate mean residence times and available groundwater quantities, the progression of pollutants and to investigate climatic effects. The "age" of groundwater is defined as the period of time between the arrival of seepage water at the groundwater table and the time of sampling.

A visualization of groundwater age in the lens was possible by changing colors of recharge water over time (Video 4, Supplementary material). By simultaneously switching all drips from one color to another, infiltration events (fronts) became visible. The layering visible in Fig. 6 is a result of a series of subsequent infiltration events. Recharge rate was maintained constant at 1.152 m d$^{-1}$ during the entire experiment. At first, a lens was generated using freshwater with uranine until equilibrium (layer 1, Fig. 6). Then we switched colors subsequently to:

- Eosine (red) for 120 min (layer 2, Fig. 6).
- Indigotine (blue) for 100 min (layer 3).
- Uranine (yellow) for 80 min (layer 4).
- Eosine (red) for 60 min (layer 5).

After the last 60 min of recharge with eosine, the photo shown in Fig. 6 was taken. An image of the age stratification within the freshwater lens became visible. A very similar pattern could be reproduced using particle tracking in the numerical model (not shown here).

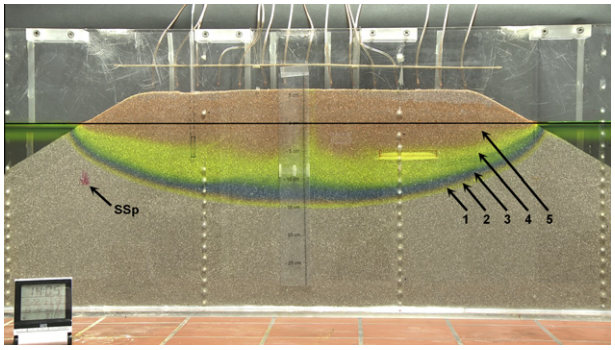


**Fig. 6.** Sand-box model visualizing age stratification of five successive infiltration events (well inactive). SSp = saltwater spot, colored.

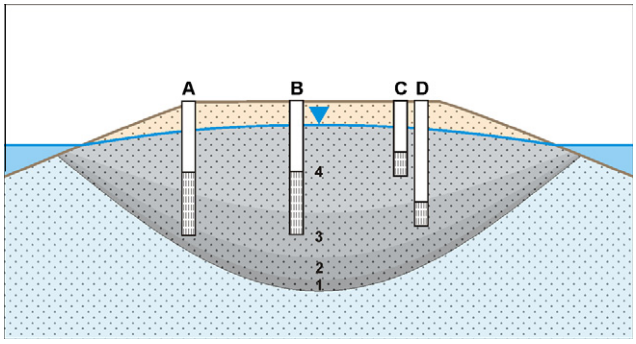


**Fig. 8.** Sketch of a freshwater lens with wells tapping groundwater at different distances from the shore (A) and (B), and with different screen depths (C) and (D). Numbers 1–4 denote layers of different times since recharge.

### 3.5. Visualization of saltwater movement

Due to the dispersive entrainment of salt water at the interface, a slow convection cell develops in the saline zone (Cooper, 1959; Reilly and Goodman, 1985; Michael et al., 2005). We injected small volumes of colored salt water with a syringe into this zone to visualize movement of salt water (Fig. 6). As expected, movement of saline water is very slow and becomes visible only close to the interface, especially at the discharge zone and around the area of upconing below a pumping well. In the latter case, the films we took trace the flow paths of salt water rising to the well (Video 4, Supplementary material).

### 3.6. Upconing under vertical and horizontal wells

We performed two physical experiments to compare the performance of a vertical and a horizontal well. We chose the parameters of the horizontal well to be as similar as possible to the vertical well to avoid a bias towards the former. With the exception of the screen being vertical or horizontal, respectively, all parameters were equal. The shafts of both wells were installed at the same distance from the "coastline". The pump, in our case simulated by the intake of the suction tube, was installed at a depth of 2.5 cm below sea level (on top or at the beginning of the screen, respectively). Screen length was 4 cm for both wells. The distance from the bottom of the screen to the undisturbed interface was 10 cm and 6 cm for the horizontal and vertical well, respectively.

The two experiments started with pumping from the vertical well and later, after complete recovery of the lens, from the horizontal well. The initial freshwater lens had a maximum thickness of 15 cm below sea level at $x = 0$. Three different pumping rates were applied for 1.5, 2.5 and 1.5 h, respectively, as indicated by the dashed lines in Fig. 8. The pumping rates for the horizontal well were 0.8 ml min$^{-1}$ higher (maximum deviation of 6%) for all three steps due to technical reasons.

For the first pumping rate, no rise in electric conductivity was observed in neither the vertical nor the horizontal well. Even though electric conductivity remained at 590 μS cm$^{-1}$ for 1.5 h of pumping, a slight rise of the interface could be visually observed in both cases. Increasing the pumping rate by around 5 ml min$^{-1}$, electric conductivity differed significantly between both wells. While the horizontal well showed a slightly elevated but almost constant conductivity of 660 μS cm$^{-1}$ after 2.5 h, the vertical well showed beginning salt water intrusion, indicated by a final conductivity of 1600 μS cm$^{-1}$. For the third pumping rate, both wells showed a clear break-through of saltwater (Fig. 7). The vertical well, however, shows a much higher proportion of saltwater intake.

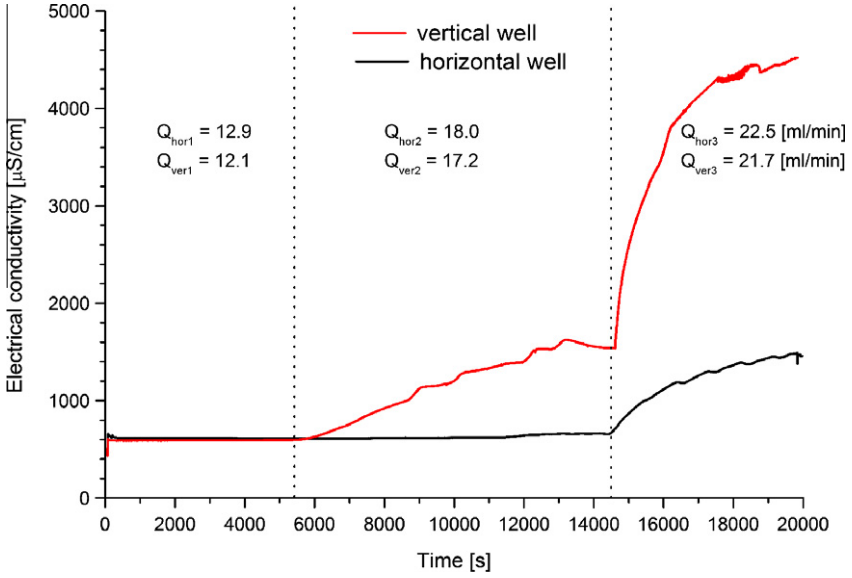


**Fig. 7.** Electric conductivity of water pumped from the horizontal (black) and the vertical well (red) showing different reactions to the applied pumping rates (changes in pumping rate indicated by dashed lines). (For interpretation of the references to colour in this figure legend, the reader is referred to the web version of this article.)

The minor fluctuations in the electric conductivity signals shown in Fig. 7 are triggered by intermittent input of saltwater. These injections were necessary to replace the pumped saltwater volume. The experiments show that a horizontal well can pump at a higher rate than a vertical well without compromising the interface.

Our results cannot be transferred directly to real world upconing due to the boundary conditions of our physical model. However, the boundary effects equally influence the horizontal and the vertical well, and therefore allow a comparison. Yet, in reality, horizontal wells are often installed at more shallow depth and often have several screens and higher pumping rates.

## 4. Discussion

Our findings, especially the travel times and the age stratification, have some interesting implications for the interpretation of groundwater ages in freshwater lenses, e.g. by isotopic analyses:

(1) A freshwater lens must not be considered a well-mixed reservoir. A non depth-specific sample from a long well screen includes unknown proportions of water of different residence times, yielding a mixed age of no real value, especially if no flow model is available. Two identical wells (same screen depth and length, same pumping rate) may yield completely different residence times depending on their position on the island (wells A and B, Fig. 8). A well close to the middle may predominantly tap from the thick layer of young water present there while a well close to the coast may tap various age zones due to the vertical movement close to the discharge zone.
(2) The thickness of the discrete layers (infiltration events), visualized by different tracer colors, decreases over time. The proportion of young water in the water column is higher than that of older water. Wells C and D show the effect on the age of pumped water (Fig. 8).
(3) All water layers remain in contact with the discharge zone at all times until they are completely squeezed out or mixed away at the interface through dispersion and diffusion. As an example, the thin eosine layer close to the interface (Fig. 6) was recharged for 120 min, while the eosin layer close to the surface was recharged for only 60 min. The "age" of groundwater at the bottom of the lens gives an estimate of the maximum travel time but not of the age of the formation of the lens itself. Older layers may have been "squeezed out" already.
(4) The proportions of water of different residence times pumped from the screen of a well depend on the depth and length of the screened interval, the hydraulic conductivity of the layers and the position of the pump (e.g. Houben and Hauschild, 2011).
(5) The age stratification of the water column may include layers of different recharge rates or even one or more hiatus, e.g. caused by dry years with low or even no recharge. The duration of the dry period must of course not exceed the time necessary to completely degrade the lens.
(6) The calculation of travel times based on models of the hydraulic flow regime, is a necessary prerequisite to validate groundwater ages derived from radionuclide tracers, such as tritium or radiogenic carbon.

## 5. Conclusions

In our physical experiments we used for the first time time-dependent applications of artificial tracers to visualize internal flow processes, like flow paths and age stratification, in a two dimensional cross section of a freshwater lens. The physical model results for steady state lens thickness, formation and degeneration, travel times and age stratification were successfully compared to numerical and, if applicable, analytical model calculations.

Particularly, this study has shown that investigations of groundwater age and residence times within a freshwater lens can only be interpreted with the understanding of the flow regime. This imposes restrictions on the sampling of water for age dating, e.g. samples need to be depth-specific in order to yield useful results.

The flow paths and travel times find their practical application in the delineation of protection zones, e.g. the 50-day zone which is intended to prevent fecal bacteria from entering a well. They can also be used to predict the degradation of pollutants, if kinetic rate laws are known, and the propagation of radionuclide tracers such as tritium.

Our findings also have some practical implications for sustainable water resource management, e.g. the sustainable pumping rate of wells. By our experiments we could show that a horizontal well with the same screen depth and distance to shore allows a higher sustainable yield than a vertical well.

Anisotropy and geological heterogeneities which were not considered in our experiments may significantly disturb the flow field and will cause deviations from the continuous age stratification. Further investigations will focus on lens dynamics in layered systems, variations of island morphology and artificial groundwater recharge.

## Acknowledgements

We thank the State Authority for Mining, Energy and Geology (LBEG) of Lower Saxony, Hannover, for allocating the physical model. The authors also thank Thomas Himmelsbach, Thomas Graf, Hartmut Holländer, Hans Sulzbacher and Axel Suckow for helpful discussions. The support of Stefan Löffler for the experimental work is gratefully acknowledged. We also like to thank Berndt Assmann and Ulrich Gersdorf for their help in the elaboration of Figs. 1 and 8 and Bernd Gibadlo for his assistance in the preparation of the film documentation. Finally, the helpful comments by Pieter Stuyfzand and another anonymous reviewer are gratefully acknowledged.

## Appendix A. Supplementary material

Supplementary data associated with this article can be found, in the online version, at http://dx.doi.org/10.1016/j.jhydrol.2012.05.070.

## References

Abdollahi-Nasab, A., Boufadel, M.C., Li, H., Weaver, J.W., 2010. Saltwater flushing by freshwater in a laboratory beach. J. Hydrol. 836, 1–12.
Bailey, R.T., Jenson, J.W., Olsen, A.E., 2009. Numerical modeling of atoll island hydrogeology. Ground Water 47 (2), 184–196.
Barrett, B., Heinson, G., Hatch, M., Telfer, A., 2002. Geophysical methods in saline groundwater studies: locating perched water tables and fresh-water lenses. Explor. Geophys. 33 (2), 115–121.
Baydon-Ghyben, W., 1898. Nota in verband met de voorgenomen putboring nabij Amsterdam. Koninglijk Instituut Ingenieurs Tijdschrift 1888–1889, 8–22.
Bear, J., Cheng, A.-H.D., Sorek, D., Ouazar, D.S., Herrera, I., 2010. Seawater Intrusion in Coastal Aquifers – Concepts, Methods and Practices. Springer, Berlin, 640p.
Beyer, W., Schweiger, K.H., 1969. Zur bestimmung des entwässerbaren porenanteils der grundwasserleiter. Wasserwirtschaft-Wassertechnik 19 (3), 57–60.
Chesnaux, R., Allen, D.M., 2008. Groundwater travel times for unconfined island aquifers bounded by freshwater or seawater. Hydrogeol. J. 16, 437–445.
Cooper, H.H., 1959. A hypothesis concerning the dynamic balance of fresh water and salt water in a coastal aquifer. J. Geophys. Res. 64 (4), 461–467.
Cooper, H.H., Kohout, F.A., Henry, H.R., Glover, R.E., 1964. Seawater in coastal aquifers US. Geol. Surv. Water-Suppl. Pap. 1613-C, 84.
Dagan, G., Bear, J., 1968. Solving the problem of local interface upconing in a coastal aquifer by the method of small perturbations. J. Hydraul. Res. 6, 15–44.

Diersch, H.-J.G., 2005. FEFLOW: Finite Element Subsurface Flow and Transport Simulation System. WASY GmbH Institute for Water Resources Planning and Systems Research, Berlin, 292p.
Fetter, C.W., 1972. Position of the saline water interface beneath oceanic islands. Water Resour. Res. 8, 1307–1314.
Goswami, R.R., Clement, T.P., 2007. Laboratory-scale investigation of saltwater intrusion dynamics. Water Resour. Res. 43 (4), W04418. http://dx.doi.org/10.1029/2006WR005151.
Gupta, D.A., Gaikwad, V.P., 1988. Interface upconing due to a horizontal well in unconfined aquifer. Ground Water 25 (4), 466–474.
Herzberg, A., 1901. Die wasserversorgung einiger nordseebäder. J. Gasbeleuchtung Wasserversorgung 44, 815–819.
Houben, G., Hauschild, S., 2011. Numerical modeling of the near-field hydraulics of water wells. Ground Water 49 (4), 570–575.
Jakovovic, D., Werner, A.D., Simmons, C.T., 2011. Numerical modeling of saltwater up-coning: comparison with experimental laboratory observations. J. Hydrol. 402, 261–273.
Luyun, R., Momii, K., Nakagawa, K., 2011. Effects of recharge wells and flow barriers on seawater intrusion. Ground Water 49 (2), 239–249.
Maas, K., 2007. Influences of climate change on a Ghijben-Herzberg lens. J. Hydrol. 347, 223–228.
Michael, H.A., Mulligan, A.E., Harvey, C.F., 2005. Seasonal oscillations in water exchange between aquifers and the coastal ocean. Nature 436, 1145–1148.
Oberdorfer, J.A., Hogan, P.J., Buddemeier, R.W., 1990. Atoll island hydrogeology: flow and freshwater occurrence in a tidally dominated system. J. Hydrol. 120, 327–340.
Oswald, S.E., Kinzelbach, W., 2004. Three-dimensional physical benchmark experiments to test variable-density flow models. J. Hydrol. 290, 22–42.
Oude Essink, G.H.P., 1996. Impacts of Sea Level Rise on Groundwater Flow Regimes; A Sensitivity Analysis for the Netherlands. PhD Thesis Technical Univ. Delft, Netherlands, 411p.
Oude Essink, G.H.P., van Baaren, E.S., de Louw, P.G.B., 2010. Effects of climate change on six coastal groundwater systems: a modeling study in the Netherlands. Water Resour. Res. 46, W00F04 doi:10.1029/2009WR008719.
PAI, 2006. Population Action International. <http://www.earth.columbia.edu/news/2006/story07-11-06.ph>.
Pennink, J.M.K., 1915. Grondwater Stroombanen. Stadsdrukkery Amsterdam. <http://www.citg.tudelft.nl/index.php?id=19739&L=1>.
Reilly, T.E., Goodman, A.S., 1985. Quantitative analysis of saltwater–freshwater relationships in groundwater systems – a historical perspective. J. Hydrol. 80, 125–160.
Schmorak, S., Mercado, A., 1969. Upconing of freshwater–seawater interface below pumping wells. Water Resour. Res. 5, 1290–1311.
Shi, L., Cui, L., Park, N., Huyakorn, P.S., 2011. Applicability of a sharp-interface model for estimating steady-state salinity at pumping wells-validation against sand tank experiments. J. Contam. Hydrol. 124, 35–42.
Siemon, B., Christiansen, A.V., Auken, E., 2009. A review of helicopter-borne electromagnetic methods for groundwater exploration. Near Surf. Geophys. 7 (5–6), 629–646.
Simmons, C.T., Pierini, M.L., Hutson, J.L., 2002. Laboratory investigation of variable-density flow and solute transport in unsaturated–saturated porous media. Transp. Porous Media 47, 215–244.
Stuyfzand, P.J., Bruggeman, G.A., 1994. Analytical approximations for fresh water lenses in coastal dunes. In: Proc. 13th Salt Water Intrusion Meeting, Cagliari, Italy, June 1994. pp. 15–33.
Tronicke, J., Blindow, N., Groß, R., Lange, M.A., 1999. Joint application of surface electrical resistivity- and GPR-measurements for groundwater exploration on the island of Spiekeroog – Northern Germany. J. Hydrol. 223, 44–53.
Vacher, H.L., 1988. Dupuit-Ghyben-Herzberg analysis of strip-island lenses. Geolog. Soc. Am. Bul. 100, 580–591.
Vacher, H.L., Bengtsson, T.O., Plummer, L.N., 1990. Hydrology of meteoric diagenesis: residence time of meteoric ground water in island fresh-water lenses with application to aragonite-calcite stabilization rate in Bermuda. Geolog. Soc. Am. Bul. 102 (2), 223–232.
Van der Veer, P., 1977. Analytical solution for a two-fluid flow in a coastal aquifer involving a phreatic surface with precipitation. J. Hydrol. 35, 271–278.
Werner, A.D., Jakovovic, D., Simmons, C.T., 2009. Experimental observations of saltwater up-coning. J. Hydrol. 373, 230–241.
Werner, A.D., Bakker, M., Post, V.E.A., Vandenbohede, A., Lu, C., Ataie-Ashtiani, B., Simmons, C.T., Barry, D.A., in press. Seawater intrusion processes, investigation and management: recent advances and future challenges. Adv. Wat. Res.
White, I., Falkland, T., 2010. Management of freshwater lenses on small pacific islands. Hydrogeol. J. 18 (1), 227–246.
Zhang, Q., Volker, R.E., Lockington, D.A., 2002. Experimental investigation of contaminant transport in coastal groundwater. Adv. Environ. Res. 6, 229–237.
Zhao, J., WenZhong, H., ShuLong, C., Zhen, L., ZhouCong, Z., LiuLi, H., 2009. A Laboratory Model of the Evolution of an Island Freshwater Lens. IAHS Press, Hyderabad, pp. 154–161.
Zhou, Q., Bear, J., Bensabat, J., 2005. Saltwater upconing and decay beneath a well pumping above an interface zone. Transp. Porous Media 61 (3), 337–363.